Report no. 95/03

Analysis of the Accuracy of Shock-Capturing in the Steady Quasi-1D Euler Equations

M. B. Giles
Oxford University Computing Laboratory
Numerical Analysis Group

Insight into the accuracy of steady shock-capturing CFD methods is obtained through analysis of a simple problem involving steady transonic flow in a quasi-1D diverging duct. It is proved that the discrete solution error on either side of the shock is $O(h^n)$ where n is the order of accuracy of the conservative finite volume discretisation. Furthermore, it is shown that provided that $n \geq 2$ then the error in approximating $\int p\,dx$ is $O(h^2)$. This result is in contrast to the general belief that shocks in 2D and 3D Euler calculations lead to first order errors, which motivates much of the research into grid adaptation methods.

Subject classifications: AMS(MOS): 65N15, 76-08, 76N10

Key words and phrases: CFD, compressible flow, finite volume, error analysis

This work was supported by Rolls-Royce plc and the Department of Mechanical and Aerospace Engineering, Princeton University.

Oxford University Computing Laboratory
Numerical Analysis Group
Wolfson Building
Parks Road
Oxford, England OX1 3QD
E-mail: giles@comlab.oxford.ac.uk

April, 1997

1 Introduction

The paper by Jameson, Schmidt and Turkel [5] is a landmark in the development of CFD methods, being one of the first papers on the solution of the multidimensional Euler equations in conservative form by a time-marching method. Runge-Kutta time-marching methods, in conjunction with multigrid for steady-state applications [2], are now the mainstay of Euler and Navier-Stokes calculations. One of the key advantages of these methods over the potential flow methods which they have largely replaced is the ability to treat supersonic and transonic flow with shocks of arbitrary strength. The importance of shocks in the aeronautical applications which have been the driving motivation for Jameson's research has led to the development of grid adaptation, in which the discrete shock width is reduced by adaptively reducing the size of cells crossed by the shock. With structured grids this is usually accomplished by redistributing the grid nodes. With unstructured grids, in which Jameson has again played a pioneering role [3, 4], it is usually accomplished by grid refinement, subdividing triangles or tetrahedra into a number of smaller triangles or tetrahedra.

One important aspect of grid adaptation is the criterion used to decide which which cells are adapted. Ideally, the criterion (or a combination of criteria) will lead to the adaptation of only those cells in which large flow gradients generate large numerical errors. Unfortunately, there is no complete theory of *a posteriori* error estimation for the discretisation of nonlinear p.d.e.'s on which to base rigorous adaptation criteria and so they have instead been developed based on a combination of model linear p.d.e.'s, engineering intuition and practical experience (e.g. [6, 7, 8, 1, 9]). One typical adaptation parameter that is used is

$$A_p = h|\delta p| \tag{1.1}$$

where h is some measure of the cell length, and δp is a first difference of the pressure field. At shocks, δp is independent of the cell size and so the shock cells are adapted repeatedly until h is sufficiently small that A_p falls below the adaptation threshold. Away from shocks,

$$A_p \approx h^2|\nabla p| \tag{1.2}$$

and so the adapted grid resolution is related to the flow gradient, as desired.

In designing adaptation criteria such as this which will generate a large number of adapted cells at shocks and so obtain very thin discrete shocks, it is implicitly assumed that the shock would otherwise cause substantial numerical errors. The lift on a wing is one of the most important engineering quantities obtained from a solution of the Euler equations. For such a calculation it appears, intuitively, that since the shock is 'smeared' over one or two cells there must be an error in the lift prediction of order $h_s \Delta p$ where h_s is the cell size at the shock and Δp is the jump in pressure across the shock. This appears to be the basis

for the particular adaptation criterion above, but other adaptation criteria also lead to very substantial refinement of shock cells and so the belief in a significant first order error at shocks seems widespread although not stated.

The research in this paper arose from discussions with Antony Jameson about this issue of shock-generated errors. His experience with uniform grid refinement studies for a variety of test cases with a number of different numerical algorithms, does not support the hypothesis of a first order lift error. Almost all show convergence in lift and drag to be faster than first order. A substantial fraction, but not the majority, show second order convergence with the error proportional to h^2. The majority show very rapid convergence which does not appear to be proportional to h^m for any value of m; in many cases the convergence is not even monotonic. Thus, other than refuting the idea of a clear first order error due to the shock, the empirical evidence is unclear.

To gain insight into this behaviour, section 2 performs a numerical analysis of shock-capturing discretisations of the Euler equations for a model problem, transonic quasi-1D flow in a diverging duct. The analysis shows that the error in the 'lift' prediction is in fact $O(h^2)$, not $O(h)$. Furthermore, it reveals the possible origin of the non-monotonic convergence observed in 2D and 3D calculations. Section 3 presents numerical results for a particular numerical method with the adaptive smoothing often used by Jameson; these results confirm the findings of the numerical analysis. The final section discusses the conclusions that can be drawn from the work.

2 Analysis

2.1 Analytic equations

The steady quasi-1D Euler equations in conservative form are

$$\frac{d}{dx}(AF) - \frac{dA}{dx}P = 0, \tag{2.1}$$

where U is the conservation state vector

$$U = \begin{pmatrix} \rho \\ \rho u \\ \rho E \end{pmatrix}, \tag{2.2}$$

F is the flux vector

$$F = \begin{pmatrix} \rho u \\ \rho u^2 + p \\ \rho u H \end{pmatrix}, \tag{2.3}$$

and P has the contribution of the pressure on the side-wall

$$P = \begin{pmatrix} 0 \\ p \\ 0 \end{pmatrix}. \tag{2.4}$$

$A(x)$ is the cross-sectional area of the duct which, for convenience, is assumed to be locally constant at the two ends.

At the supersonic inflow at $x=0$ the entire state vector $U(0)$ is specified. At the subsonic outflow at $x=1$, one quantity is specified since there is one characteristic wave travelling upstream. This quantity could be the static pressure, but the precise choice is not important.

Integration of Eq. (2.1) yields

$$[AF]_{x_0}^{x_1} = \int_{x_0}^{x_1} \frac{dA}{dx} P \, dx, \tag{2.5}$$

for any arbitrary pair x_0, x_1. This is the integral form of the quasi-1D Euler equations and it is this form which remains valid when shocks are present. Taking $x_0=0, x_1=1$ gives

$$[AF]_0^1 = \int_0^1 \frac{dA}{dx} P \, dx = \begin{pmatrix} 0 \\ D \\ 0 \end{pmatrix}, \tag{2.6}$$

where

$$D = \int_0^1 p \frac{dA}{dx} \, dx. \tag{2.7}$$

The first and third components of Eq. (2.6) together with the one outflow boundary condition totally specify the three components of $U(1)$ given that $U(0)$ has already been specified. The second component of Eq. (2.6) then defines D uniquely as a function of the boundary conditions independent of the precise variation of $p(x)$ or $A(x)$ between the end points. This is the key result which will be used in determining the accuracy with which the discretisation approximates the quantity

$$\int_0^1 p \, dx \tag{2.8}$$

which represents the lift in 2D and 3D Euler calculations for lifting bodies.

2.2 Discrete equations

The analysis considers steady discrete equations with the following conservative form

$$A_{j+1/2} F^h_{j+1/2} - A_{j-1/2} F^h_{j-1/2} = \Delta A_j P^h_j, \qquad \Delta A_j \equiv A_{j+1/2} - A_{j-1/2}. \tag{2.9}$$

Both the discrete flux $F^h_{j-1/2}$ and the sidewall term P^h_j are functions of the neighbouring values of the state vector U^h_j,

$$F^h_{j-1/2} = F^h(U^h_{j-m-1}, ..., U^h_{j-1}, U^h_j ... U^h_{j+m}), \quad P^h_j = P^h(U^h_{j-m}, ..., U^h_j, ... U^h_{j+m}) \tag{2.10}$$

with the consistency requirement that

$$U^h_j = U_{const} \implies F^h_{j-1/2} = F(U_{const}), \quad P^h_j = P(U_{const}). \tag{2.11}$$

Many quasi-1D schemes are of this form, including the flux-vector splitting scheme of van Leer, the flux-difference splitting scheme of Roe, and Jameson's cell-centred central differencing scheme with added artificial viscosity terms.

The computational grid is taken to be uniform with mesh spacing h, and the order of accuracy of the finite volume discretisation is $O(h^n)$ as determined by a standard truncation error analysis assuming the solution is differentiable.

Summing the discrete equations over the entire computational domain yields

$$A_{J+1/2} F^h_{J+1/2} - A_{1/2} F^h_{1/2} = \sum_1^J \Delta A_j \, P^h_j = \begin{pmatrix} 0 \\ D^h \\ 0 \end{pmatrix}, \tag{2.12}$$

where

$$D^h = \sum_1^J \Delta A_j \, p^h_j. \tag{2.13}$$

This is very similar to the integral equation satisfied by the analytic solution and it has similar consequences.

The restriction that $A(x)$ is locally constant at each end of the domain ensures that the discrete solution U^h_j also approaches a uniform state at each end. Analysis of linear perturbations to the discrete solution for a constant area duct show that such perturbations decay exponentially with a length scale proportional to the grid spacing h. Therefore there exist state vectors $U^h(0)$ and $U^h(1)$ and constants c_1, c_2 such that

$$\begin{aligned} U^h_j &= U^h(0) + o(e^{-c_1/h}), \qquad j \le 2m \\ U^h_j &= U^h(1) + o(e^{-c_2/h}), \qquad j \ge J - 2m \end{aligned} \tag{2.14}$$

with m being the span of the discrete flux function as previously defined. Therefore, using the consistency of the discrete fluxes it follows that

$$A(1)F(U^h(1)) - A(0)F(U^h(0)) = \begin{pmatrix} 0 \\ D^h \\ 0 \end{pmatrix} + o(e^{-c/h}) \tag{2.15}$$

The inflow boundary conditions ensure that $U^h(0) = U(0)$. The first and third components of the above equation together with the specification of the correct

exit pressure then ensure that $U^h(1) = U(1) + o(e^{-c/h})$. The second component then implies that

$$D^h = D + o(e^{-c/h}). \tag{2.16}$$

In addition, the fact that the boundary data is exponentially accurate and the finite volume discretisation has accuracy $O(h^n)$ means that away from the shock the solution error is $O(h^n)$. At the shock the pointwise error will be $O(1)$ but linear perturbation analysis agains shows that this component will decay exponentially away from the shock so that the composite solution error can be represented as

$$U_j^h \;=\; U(x_j) + O(h^n, e^{-c_3|x_j - x_s|/h}) \;=\; U(x_j) + O(h^n, e^{-c_3|j-s|}) \tag{2.17}$$

where s is the index of the cell containing the analytic shock, and c_3 is another constant.

2.3 Accuracy of lift integral

Defining p_j to be the average analytic pressure in cell j,

$$p_j = h^{-1} \int_{x_{j-1/2}}^{x_{j+1/2}} p \, dx, \tag{2.18}$$

the objective is to quantify the error in approximating the lift integral,

$$L^h - L = h \sum p_j^h - \int_0^1 p \, dx = h \sum (p_j^h - p_j). \tag{2.19}$$

The first step is to express D in terms of the average analytic pressures within each cell. In the cell containing the analytic shock, $\frac{dA}{dx}$ is differentiable and so

$$\int_{x_{j-1/2}}^{x_{j+1/2}} p \frac{dA}{dx} \, dx = p_j \Delta A_s + O(h^2), \tag{2.20}$$

with ΔA_s denoting the area change in the shock cell. In all other cells, p is also differentiable and so

$$\int_{x_{j-1/2}}^{x_{j+1/2}} p \frac{dA}{dx} \, dx = p_j \Delta A_j + O(h^3). \tag{2.21}$$

Hence, summing over all cells,

$$D = \sum p_j \Delta A_j + O(h^2). \tag{2.22}$$

From Eq. (2.16) it can then be concluded that

$$\sum (p_j^h - p_j) \Delta A_j = O(h^2). \tag{2.23}$$

The second step is to relate the average analytic pressure to the discrete pressure. In all cells other than the shock cell,

$$p_j = p(x_j) + O(h^2) \tag{2.24}$$

and so provided that the order of accuracy $n \geq 2$, it follows from Eq. (2.17) that

$$p_j^h = p_j + O(h^2, e^{-c_3|j-s|}). \tag{2.25}$$

Also, since $\frac{dA}{dx}$ is differentiable,

$$\Delta A_j = \Delta A_s + O(h^2|j-s|) \tag{2.26}$$

Combining these gives

$$\sum (p_j^h - p_j)(\Delta A_j - \Delta A_s) = O(h^2) \tag{2.27}$$

since

$$\sum h^4|j-s| = O(h^2), \qquad \sum h^2|j-s|e^{-c|j-s|} = O(h^2) \tag{2.28}$$

The final step is to combine Eqs. (2.23,2.27) to give

$$\begin{aligned} h^{-1}\Delta A_s(L^h - L) &= \Delta A_s \sum (p_j^h - p_j) \\ &= \sum (p_j^h - p_j)\Delta A_j - \sum (p_j^h - p_j)(\Delta A_j - \Delta A_s) \\ &= O(h^2) \end{aligned} \tag{2.29}$$

and so

$$L^h - L = O(h^2) \tag{2.30}$$

since $\frac{dA}{dx}$ must be non-zero at the shock for the shock position to be well-determined.

Note that there is nothing in the above analysis to suggest that the quantity C^h, defined by

$$C^h = h^{-2}(L^h - L), \tag{2.31}$$

should asymptote to a constant as $h \to 0$. The proven second order accuracy only requires that C^h be bounded. In fact, it is possible that C^h will vary if one uses a sequence of increasingly fine grids, depending on the location of the shock relative to the grid. If x_s is the shock location, and as before x_s^h is the centre of the cell containing the shock then C^h is likely to be a function of the parameter,

$$\lambda = h^{-1}(x_s - x_s^h) \tag{2.32}$$

which will vary from grid to grid. The variation is likely to be greatest for methods which produce very sharp shocks, e.g. flux-vector splitting, and least for methods which produce more smeared shocks for which the relative grid location is much less important. In this latter case, if C^h is relatively constant it may even be possible to use Richardson extrapolation to obtain higher accuracy.

3 Numerical results

Numerical results have been obtained for a discretisation of the form specified in the last section. Dropping the superscript h used in the last section to denote the discrete variables, the pressure on the sidewall is given by

$$P_j = \tfrac{1}{4}\,(\,P(U_{j+1}) + 2\,P(U_{j+1}) + P(U_{j-1})\,) \tag{3.1}$$

and the discrete flux is

$$\begin{aligned} F_{j+\frac{1}{2}} &= \tfrac{1}{2}\,(F(U_{j+1}) + F(U_j)) + \epsilon^{(2)}_{j+\frac{1}{2}}\lambda_{j+\frac{1}{2}}\,(U_{j+1} - U_j) \\ &\quad + \epsilon^{(4)}_{j+\frac{1}{2}}\lambda_{j+\frac{1}{2}}\,(U_{j+2} - 3U_{j+1} + 3U_j - U_{j+1})\,. \end{aligned} \tag{3.2}$$

The maximum characteristic velocity λ is given by

$$\lambda_{j+\frac{1}{2}} = \tfrac{1}{2}\,(|u_{j+1}| + c_{j+1} + |u_j| + c_j) \tag{3.3}$$

where u and c are the convection velocity and speed of sound, respectively. The coefficients $\epsilon^{(2)}$ and $\epsilon^{(4)}$ are defined adaptively based on the non-dimensional pressure switch

$$s_j = \left|\frac{p_{j+1} - 2p_j + p_{j-1}}{p_{j+1} + 2p_j + p_{j-1}}\right| \tag{3.4}$$

to obtain second difference smoothing in the shock region, but only fourth difference smoothing in the smooth flow regions

$$\begin{aligned} \epsilon^{(2)}_{j+\frac{1}{2}} &= B\,\min(0.5,\,\max(s_{j+2}, s_{j+1}, s_j, s_{j-1})) \\ \epsilon^{(4)}_{j+\frac{1}{2}} &= \max(0,\,0.25 - 2\epsilon^{(2)}_{j+\frac{1}{2}}). \end{aligned} \tag{3.5}$$

The nondimensional constant B controls the degree of smearing of the shock. Calculations were performed for both $B = 1$ giving fairly crisp shocks with one or two interior points, and $B = 5$ giving shocks which are more smeared with approximately six interior points.

The duct width $A(x)$ is defined as

$$A(x) = \begin{cases} 1.0304, & x \le 0 \\ 1.0304 + 0.0718x^3(10 - 15x + 6x^2) - 0.9482x^3(1-x)^3, & 0 < x < 1 \\ 1.1022, & x \ge 1 \end{cases} \tag{3.6}$$

The constants were chosen so that A, $\frac{dA}{dx}$, $\frac{d^2A}{dx^2}$ are all continuous at $x = 0$ and $x = 1$. At the inflow at $x = -0.2$ the flow is specified to be supersonic, with conditions such that

$$p_o = 1.0, \quad \rho_o = 1.0, \quad M = 1.2 \tag{3.7}$$

where p_o, ρ_o and M are the stagnation pressure, stagnation density and Mach number, respectively. The static pressure specified at the outflow boundary at $x = 1.2$ is

$$p = 0.7143. \tag{3.8}$$

These boundary conditions together with the definition of $A(x)$ lead to a shock at $x = 0.6$, with a peak Mach number of 1.3. The steady-state discrete solutions were obtained by a fully-converged Runge-Kutta time-marching procedure. Figure 1 shows the Mach number distribution for the solution near the shock using $B = 1$ and and a uniform grid of 64 points. Figure 2 has the corresponding solution for $B = 5$; the shock is clearly smeared.

To investigate the effect of mesh resolution, a sequence of grids was used with the number of grid points ranging from 64 to 192. For each grid, the influence of the shock position relative to the grid nodes was investigated by performing a number of calculations displacing the grid by an amount δx in the range $0 \leq \delta x \leq h$. The inflow and outflow boundaries are also displaced by the same amount, but since $A(x)$ is locally constant at each end this does not affect the results. For each calculation, the discrete lift was computed, as well as the error relative to the 'exact' lift (estimated by extrapolation from the solutions on the finest grids). Figure 3 shows the errors in lift obtained from the solutions with $B = 1$. The 'error bar' indicates the range of values obtained depending on the position of the shock relative to the grid points. Figure 4 plots the magnitude of these error bars $L^h_{max} - L^h_{min}$. Note that in both figures the quantities are plotted against h^2, not h. The linear behaviour in Figure 4 shows corresponds to the analysis in the previous section, with C^h being a function of the shock position. Figure 3 also shows an almost linear behaviour for small values of h, but for larger values the error increases more rapidly, indicating an additional error term which is $O(h^3)$, possibly due to the numerical smoothing in the smooth flow regions. Figure 3 also shows the possibility for non-monotonic convergence as h is refined; for sufficiently small values of h there are some points within the error bar which show an overprediction of the lift, while other show an underprediction. Figures 5 and 6 show the corresponding results for $B = 5$. The lift errors are now much larger but the error bars are smaller in both relative and absolute terms.

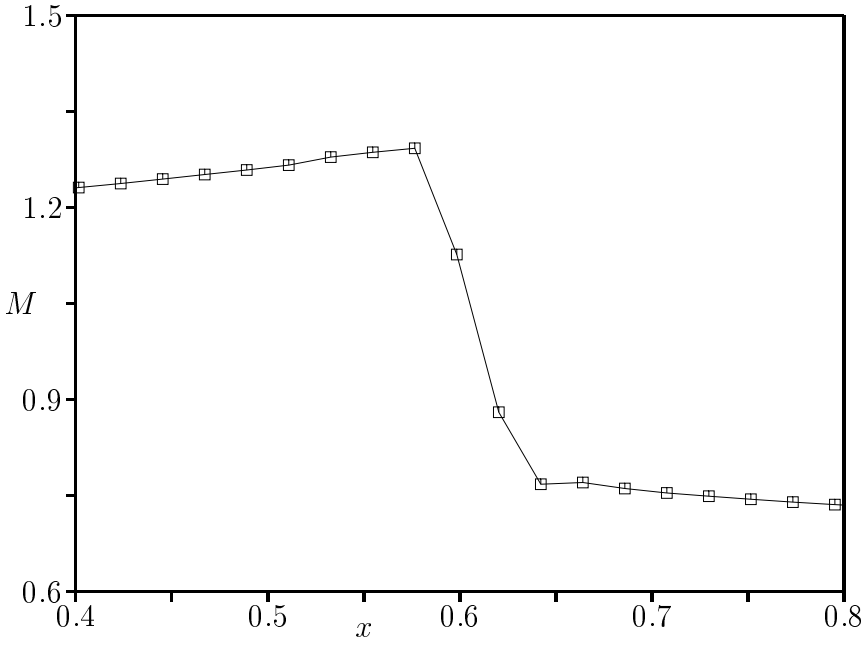

Figure 1: Mach number distribution near the shock computed using $B=1$

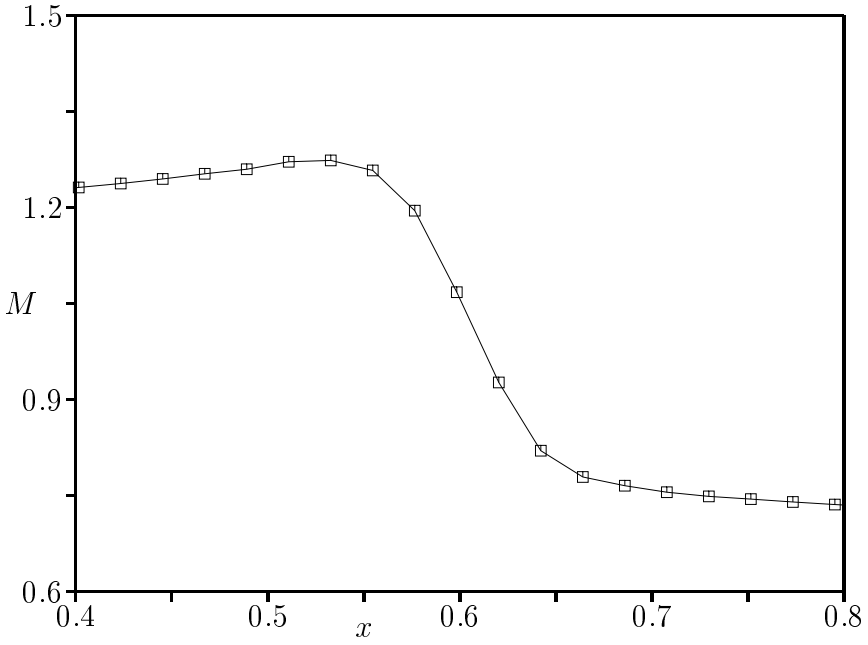

Figure 2: Mach number distribution near the shock computed using $B=5$

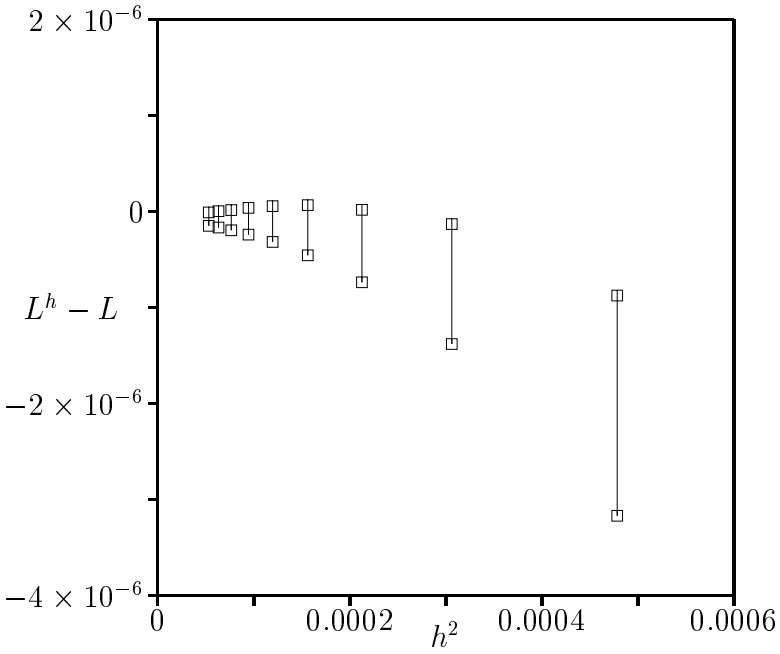

Figure 3: Lift error for results using $B = 1$

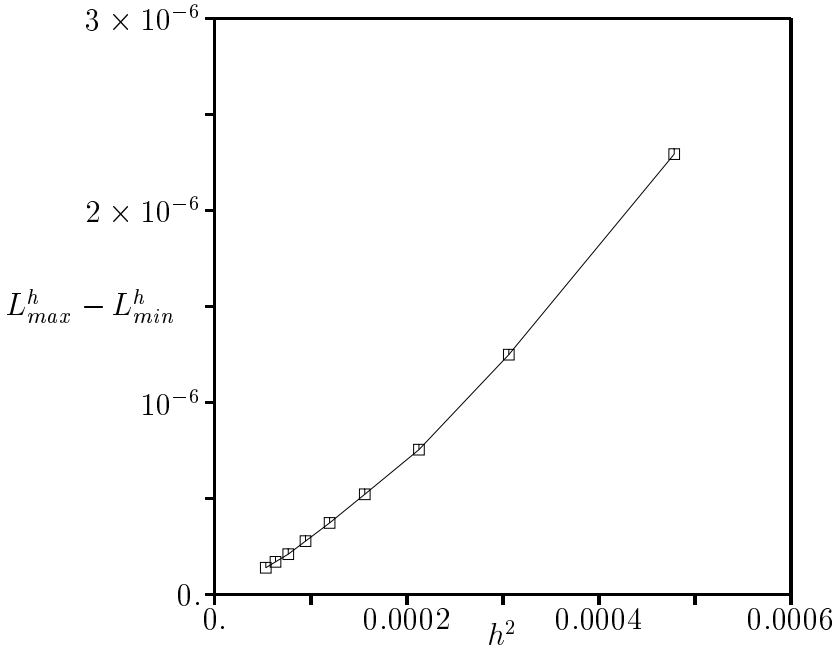

Figure 4: Lift variation for results using $B = 1$

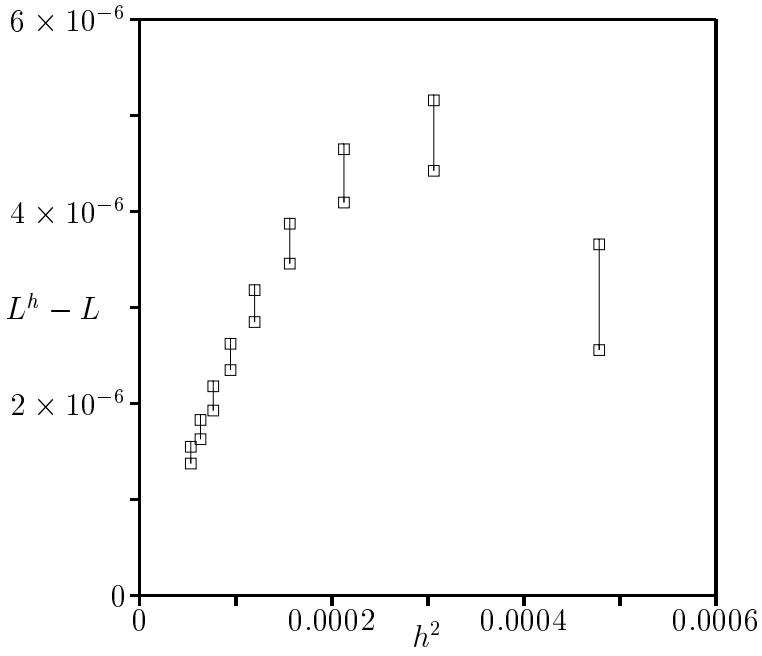

Figure 5: Lift error for results using $B = 5$

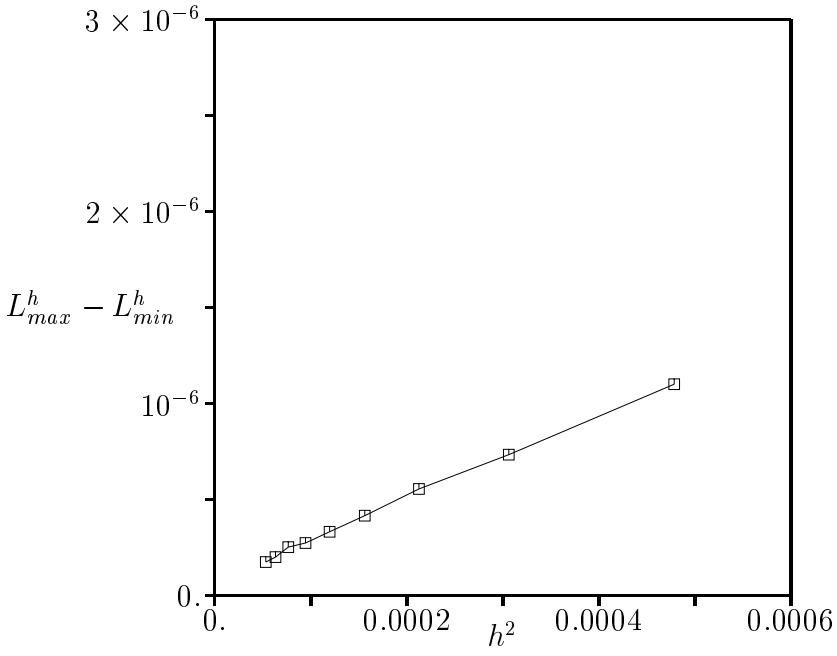

Figure 6: Lift variation for results using $B = 5$

4 Discussion

The result that the lift is determined with second order accuracy for the model quasi-1D problem is surprising and counter-intuitive. Any form of numerical integration of the analytic pressure at the discrete grid points, $p(x_j)$, will inevitably incur an integration error which is $O(h\Delta p)$, where Δp is the pressure jump across the shock. Thus, the discrete pressure values p_j^h in the neighbourhood of the shock must have a pointwise error which is $O(1)$ and of exactly the correct magnitude to cancel out this $O(h)$ error in the lift integration.

There is obviously a question about the relevance of the quasi-1D model problem to the 2D and 3D computations which are of real engineering interest. Jameson's 2D and 3D computations do behave similarly to the quasi-1D computations in this paper, which is a favourable indication. Extending the rigorous numerical analysis from the quasi-1D duct problem to a fully 2D airfoil problem is extremely challenging. Additional careful grid refinement studies with other test cases and numerical algorithms may be the only practical approach to resolving this issue of the errors due to shocks in 2D and 3D computations.

If additional empirical evidence supports the hypothesis that the shock does not generate a first order error, or even if it shows a first order error but with a coefficient very much smaller than the pressure jump Δp suggested intuitively, then it will have important consequences for grid adaptation. The present techniques assume, implicitly, a large first order error at shocks, and then aim to reduce its magnitude by reducing the cell size h at the shock. In the process, the number of cells in the shock region increases dramatically. This is particularly true in 3D when using Delauney triangulation methods which prevent the generation of stretched tetrahedra and so lead to the grid resolution along the shock being comparable to the grid resolution across the shock. If the shock does not generate large errors, then the additional computational resources will be better devoted to a more uniform adaptation of the grid, adapting all cells in the smooth flow regions in which the flow gradients are large relative to the cell size.

In viscous calculations, it can be argued with justification that the foot of the shock needs to be very accurately resolved to obtain the correct shock/boundary layer interaction. This is critical in determining both viscous losses and the boundary layer displacement thickness which affects the external inviscid flow and hence the overall pressure distribution. However, an accurate calculation of the shock/boundary layer interaction is unlikely to require that the shock is well resolved far from the wall, and so again the results in this paper suggest that considerable computational savings may be achieved by better adaptation criteria.

References

[1] J.F. Dannenhoffer, III. A comparison of two adaptive grid techniques. In *Numerical Grid Generation in Computational Fluid Mechanics*. Pineridge Press Ltd, 1988.

[2] A. Jameson. Solution of the Euler equations by a multigrid method. *Applied Mathematics and Computation*, 13:327–356, 1983.

[3] A. Jameson, T.J. Baker, and N.P. Weatherill. Calculation of inviscid transonic flow over a complete aircraft. AIAA Paper 86–0103, 1986.

[4] A. Jameson and D. Mavriplis. Finite volume solution of the two-dimensional Euler equations on a regular triangular mesh. *AIAA Journal*, 24(4):611–618, Apr 1986.

[5] A. Jameson, W. Schmidt, and E. Turkel. Numerical solutions of the Euler equations by finite volume methods with Runge–Kutta time stepping schemes. AIAA Paper 81-1259, 1981.

[6] R. Löhner, K. Morgan, and O. Zienkiewicz. *Adaptive grid refinement for the compressible Euler equations*, pages 281–297. John Wiley and Sons Ltd, 1986.

[7] D. Mavriplis and A. Jameson. Multigrid solution of the Euler equations on unstructured and adaptive meshes. In S. McCormick, editor, *Proceedings of the Third Copper Mountain Conference on Multigrid Methods: Lecture Notes in Pure and Applied Mathematics*. Marcel Dekker Inc, 1987.

[8] J. Peraire, M. Vahdati, K. Morgan, and O.C. Zienkiewicz. Adaptive remeshing for compressible flow computations. *J. Comput. Phys.*, 72:449–466, 1987.

[9] N.P. Weatherill, O. Hassan, M.J. Marchant, and D.L. Marcum. Adaptive inviscid flow solutions for aerospace geometries on efficiently generated unstructured tetrahedral meshes. AIAA Paper 93-3390, 1993.